The variations of VOCs based on the policy change of Omicron in traffic-hub city Zhengzhou

Bowen Zhang[1, 3], Dong Zhang[2, 3], Zhe Dong[2, 3], Xinshuai Song[1, 3], Ruiqin Zhang[1, 3], Xiao Li[1, 3,*]

[1]School of Ecology and Environment, Zhengzhou University, Zhengzhou 450001, China

[2]College of Chemistry, Zhengzhou University, Zhengzhou 450001, China

[3]Institute of Environmental Sciences, Zhengzhou University, Zhengzhou 450001, China

Abstract: Online volatile organic compounds (VOCs) were monitored before and after the Omicron policy change at an urban site in polluted Zhengzhou from December 1, 2022, to January 31, 2023. The characteristics and sources of VOCs were investigated. The daily mean concentrations of $PM_{2.5}$ and total VOCs (TVOCs) ranged from 53.5 to 239.4 µg/m³ and 15.6 to 57.1 ppbv, respectively, with mean values of 111.5 ± 45.1 µg/m³ and 36.1 ± 21.0 ppbv, respectively, throughout the period. Two severe pollution events (designated as Case 1 and Case 2) were identified in accordance with the National Ambient Air Quality Standards (NAAQS) (China's National Ambient Air Quality Standards (NAAQS) from 2012). Case 1 (December 5 to December 10, $PM_{2.5}$ daily mean = 142.5 µg/m³) and Case 2 (January 1 to January 8, $PM_{2.5}$ daily mean = 181.5 µg/m³) occurred during the infection period (when the policy of "full nucleic acid screening measures" was in effect) and the recovery period (after the policy was cancelled), respectively. The $PM_{2.5}$ and TVOCs values for Case 2 are, respectively, 1.3 and 1.8 times higher than those for Case 1. The results of the positive matrix factor modeling demonstrated that the primary source of volatile organic compounds (VOCs) during the observation period was industrial emissions, which constituted 32% of the total VOCs, followed by vehicle emissions (27%) and combustion (21%). In Case 1, industrial emissions constituted the primary source of VOCs, accounting for 32% of the total VOCs. In contrast, in Case 2, the contribution of vehicular emission sources increased to 33% and became the primary source of VOCs. The secondary organic aerosol formation potential for Case 1 and Case 2 were found to be 37.6 µg/m³ and 65.6 µg/m³, respectively. In Case 1, the largest contribution of SOAP from industrial sources accounted for the majority (63%, 23.8 µg/m³), followed by vehicular sources (18%). After the end of the epidemic and the resumption of productive activities in the society,

34   the difference in the proportion of SOA generated from various sources decreased. Most

35   of the SOAP came from solvent use and fuel evaporation sources, accounting for 32%

36   (20.9 μg/m³) and 26% (16.8 go/m³), respectively. On days with minimal pollution,

37   industrial sources and solvent use remain the main contributors to SOA formation.

38   Therefore, regulation of emissions from industry, solvent-using industries and motor

39   vehicles need to be prioritized to control the $PM_{2.5}$ pollution problem.

40

41   **Keywords: Volatile organic compounds; Pollution episode; Source apportionment; Positive**

42   **Matrix Factorization model; Secondary organic aerosol formation potential;**

1. Introduction

Volatile organic compounds (VOCs) in the atmosphere have high reactivity and can react with nitrogen oxides (NO_x) to form a series of secondary pollutants such as ozone (O_3) and secondary organic aerosol (SOA), resulting in regional air pollution (Li et al., 2019; Hui et al., 2020). The problem of O_3 pollution has been plaguing major urban agglomerations in China (Zheng et al., 2010; Li et al., 2014; Wang et al., 2017). SOA is an important component of fine particulate matter ($PM_{2.5}$) and contributes significantly to haze pollution (Liu et al., 2019). $PM_{2.5}$ remains the most significant air pollutant in many Chinese cities for years (Shao et al., 2016; Wu et al., 2016). In addition, VOCs, represented by the benzene homologues, can cause damage to kidneys, liver, and nervous system of humans when they enter the body (Zhang et al., 2018).

Studies have shown that the most common VOC components in China are alkanes, olefins, aromatic hydrocarbons, oxygenated VOCs (OVOCs), and halogenated hydrocarbons, among which alkanes are the most abundant species (Liu et al., 2020; Zhang et al., 2021a). VOCs in the atmosphere have a wide range of sources, and VOCs in different regions are affected by multiple factors such as local geography, climate, and human activities (Mu et al., 2023; Zou et al., 2023). The above reasons lead to significant regional and seasonal differences in the characteristics of VOCs (Song et al., 2021). For example, the annual average concentration of VOCs in the coastal background area of the Pearl River Delta is 9.3 ppbv. The seasonal variation trend of VOCs is high in autumn and winter and low in summer (Yun et al., 2021). In contrast, the average VOC concentration in autumn and winter in Beijing was 22.6 ± 12.6 ppbv, and the VOC concentration in the winter heating period was twice that in the autumn non-heating period (Niu et al., 2022).

Moreover, the sources of VOC components in different regions are also related to the local industrial structure and living habits. In rural areas of North China Plain in winter, it is found that the SOA formation potential (SOAP) of VOCs under low NO_x conditions is significantly higher than that under high NO_x conditions, and the increase of aromatic hydrocarbon emissions caused by coal combustion is the main reason for the higher SOAP in winter (Zhang et al., 2020). Li et al. (2022) found that the average increased concentration of acetylene was 4.8 times from autumn to winter in the Guanzhong Plain, indicating that fuel combustion during the heating period in winter has a significant impact on the composition of VOCs. In contrast, continuous

76 observations conducted by Zhou et al. (2022) in the suburbs of Dongguan in summer

77 found that industrial solvent usage, liquefied petroleum gas (LPG) and oil and gas

78 volatilization were the main sources of VOCs. The results highlighted a wide variation

79 of characteristics, sources and chemical reactions of VOCs in the atmosphere thus it is

80 necessary to investigate VOCs in different cities when formulating control measures.

81   Zhengzhou, as the capital of Henan Province, is an important transportation hub

82 and economic center in the Central Plains region. Zhengzhou is currently facing

83 significant air pollution problems, with the Air Quality Index at the bottom of the

84 national ranking of 168 cities for many years. In January 2023, for example, the number

85 of polluted days with $PM_{2.5}$ as the primary pollutant was 17, and the daily average value

86 of $PM_{2.5}$ reached   a   maximum   of   298 $\mu g/m^3$

87 (https://www.aqistudy.cn/historydata/daydata.php?city=%E9%83%91%E5%B7%9E

88 &month=202301, Accessed Jan 2024), which is almost 300% higher than the Chinese

89 daily average standard (grade II, 75 $\mu g/m^3$). The studies of VOCs were carried out in

90 Zhengzhou in recent years, which focused on the characteristics and sources of VOCs

91 during pollution episodes (Lai et al., 2024) or before the coronavirus epidemic outbreak

92 (Li et al., 2020; Zhang et al., 2021b). While some atmospheric VOCs studies involving

93 the impact of Covid-19 lockdown have been performed in India (Singh et al., 2023a),

94 in China (e.g., Pei et al., 2022; Jensen et al., 2023; Zuo et al., 2024), or with respect to

95 toluene, benzene, m/p-xylene and ethylbenzene only (e.g., Sahu et al., 2022; Singh et

96 al., 2023b), a gap persisted in the investigation of VOCs due to the impact of

97 abolishment of China's zero-policy. Furthermore, some studies have discussed the

98 impact of changes in human production activities on air pollution during and after the

99 outbreak of the coronavirus disease (e.g., Ma et al., 2022; Jiang et al., 2023; Song et al.,

100 2023), but as mentioned earlier, only a few studies with in-depth exploration of the

101 changes in VOCs and none dealing with ending the zero-Covid policy during Omicron

102 variant infection period.

103   In this study, a continuous online observation of VOCs in polluted winter at an

104 urban site was carried out, which covered the abolishment of lockdown measures in

105 Zhengzhou. The focus of this study was on pollution events in which the daily average

106 $PM_{2.5}$ concentration exceeded 75 $\mu g/m^3$ (China's Class II standard) for more than three

107 consecutive days, and any day in which the $PM_{2.5}$ concentration was less than 35 $\mu g/m^3$

108 (China's Class I standard) was considered a clean day. China lifted the zero-COVID

109 strategies, notably by announcing the '10 measures' about the optimization of COVID-

19 rules on 7 December 2022 (http://www.news.cn/politics/2022-12/07/c_1129189285.htm, Accessed Jan 2024), which led to significant changes in social activities. After that, China experiences a nationwide outbreak of COVID-19. Our research primarily concentrates on the period dominated by COVID-19 Omicron variant, where they demonstrate notable differences from the early virus strains (i.e., original SARS-CoV-2 virus and Delta) in terms of geographical transmission, the scale of the infected population, and symptom manifestation (Petersen et al., 2022; Merino et al., 2023). Zhengzhou Municipal Government in Henan Provincial People's Government Portal (www.henan.gov.cn) on October 5, 2022 issued Circular No. 139, the content of the circular is due to Zhengzhou during this period Omicron infection cases frequently, in order to prevent the spread of the epidemic hidden, and therefore to carry out the city's new coronavirus nucleic acid screening, screening scope for all residents in the city area, at the same time, closed public places Suspension of business, and to advise residents to reduce activities outside, and the content of the above notice similar to the notice continued to be issued until the Circular No. 162. The epidemic prevention and control measures in Zhengzhou changed to tin Circular No. 163 issued on December 4, 2022, restoring the opening of closed public places; Circular No. 164 issued on December 8 announced that it was no longer necessary to present health codes and nucleic acid negative certificates for the movement of people, and that centralized isolation would no longer be adopted for those who were positive for the infection. Since then, the number of people moving around Zhengzhou has increased and social production has resumed.

After the quarantine policy was lifted, people basically rested at home due to infection or fear of infection with Omicron. The resumption of normal production and life depends on herd immunization. This outbreak event is the longest in duration and the largest in number of infections since the 2020 outbreak of the novel coronavirus in Zhengzhou. It would be beneficial to investigate the impact of this event on emissions related to transportation and industrial production. This change is worth exploring in terms of its impact on transportation and industrial production emissions. Therefore, the characteristics and variations of VOCs during different periods were investigated to assess their impact on the formation of SOA and to provide data support for future pollution control policies in Zhengzhou.

2. Materials and methods

2.1 Sample collection and Chemical analysis

The online VOCs observation station is located on the roof of the Zhengzhou Environmental Protection Monitoring Center, which is in the urban area. The sampling site is close to main roads on three sides (150 m away from Funiu Road on the east side, 200 m away from Qinling Road on the west side, and connected to Zhongyuan Road on the south side), and surrounded by residential areas and commercial areas without other large nearby stationary sources. The sampling period for this study was from December 1, 2022, to January 31, 2023, which is always the most polluted period in the entire year. Apart from a brief occurrence of rain and snow on December 25, the sampling days were either sunny or cloudy. The wind speed (WS), temperature (Temp) and relative humidity (RH) during this period were 1.3 ± 0.9 m/s, 5.3 ± 3.2 ℃ and $38.9 \pm 19.0\%$), respectively, similar to the values observed in previous years in Zhengzhou. It is interesting to point out that the sampling period in the present study covered the entire infection period of Omicron in Zhengzhou, including the phase of surge in infected population (Infection period, from 2022.12.01 to 2022.12.31) and restoration of production and livelihood phase (Recovery period, from 2023.1.1 to 2023.1.31 in 2023) (Fig. S1, Chinese Center for Disease Control and Prevention, 2023).

The VOCs were measured hourly using a GC-FID/MS (TH-PKU 300 b, Wuhan Tianhong Instruments Co., China). The instrument TH-PKU300b includes electronic refrigeration ultra-low temperature pre-concentration sampling system, analysis system and system control software. The ambient VOCs in the first 5 minutes of each hour were collected by the sampling system and then entered the concentration system. Under low temperature conditions, the VOCs samples collected were frozen in the capillary capture column, and then quickly heated and resolved, so that the compounds entered the analysis system. After separation by chromatographic column, the compounds were monitored by FID and MS detectors. During the detection process, the atmospheric samples collected undergo analysis through two distinct pathways. C2-C5 hydrocarbons are analyzed using FID, while C5-C12 hydrocarbons, halocarbons, and OVOCs are analyzed with a MS detector. After excluding species with missing data exceeding 10%, the detected volatile organic compounds include 29 alkanes, 11 alkenes, 17 aromatics, 35 halocarbons, 12 OVOCs, 1 alkyne (acetylene), and 1 sulfide (CS_2) with a total of 106 compounds. A detailed description of the instrumentation can be

176   found in our previous study (Zhang et al., 2021; Shi et al., 2024; Zhang et al., 2024).

177   The instrument was calibrated per week to ensure the accuracy of VOCs by
178   injecting standard gases with a five-point calibration curve. The detection limit of C2-
179   C5 hydrocarbons ranges from 0.007 to 0.099 ppbv, other hydrocarbons are 0.004–0.045
180   ppbv, halogenated hydrocarbons 0.009-0.099 ppbv, OVOCs and other compounds of
181   0.006–0.095 ppbv. Thirty-two of the monitored VOCs had over 90% observed data
182   greater than the detection limit, and 34 had more than 50% observed data greater than
183   the detection limit.

184   Simultaneous observations at the same site were also carried out for particulate
185   matter ($PM_{2.5}$, PM_{10}), other trace gases (carbon monoxide (CO), O_3, nitric oxide (NO),
186   nitrogen dioxide (NO_2)), and meteorological data (Temperature, RH, WS, and wind
187   direction (WD)) based on 1 h resolution.

2.2 Positive Matrix Factorization (PMF) model

189   EPA PMF5.0 model was used for the quantitative source analysis of VOCs (Norris
190   et al., 2014). The principles and methods have been described in detail in previous
191   studies (Mozaffar et al., 2020; Zhang et al., 2021b). The decomposition of the PMF
192   mass balance equations is simplified as follows (Norris et al., 2014):

194
$$x_{ij} = \sum_{k=1}^{p} g_{ik}\,f_{kj} + e_{ij} \tag{1}$$

196   where x_{ij} is the mass concentration of species j measured in sample i; g_{ik} is the
197   contribution of factor k to the sample i ; f_{kj} represents the content of the jth species in
198   factor k; e_{ij} is the residual of species j in sample i; p represents the number of factors.
199   The fitting objective of the PMF model is to minimize the function Q to obtain the
200   factor contributions and contours. The formula for Q is given in Eq. (2):

202
$$Q = \sum_{i=1}^{n} \sum_{j=1}^{m} \left[\frac{x_{ij} - \sum_{k=1}^{p} g_{ik}f_{kj}}{u_{ij}} \right]^2 \tag{2}$$

204   where n and m denote the number of samples and VOC species, respectively.

205   Concentrations and uncertainty data are required for the PMF model. In this study,

206   the median concentration of a given species is used to replace missing values with an

207   uncertainty of four times of the median values; data less than the Method Detection

208   Limit (MDL) were replaced with half the MDL, with an uncertainty of 5/6 of the MDL;

209   and the uncertainty for values greater than the MDL was calculated using Eq. (3). In

210   Eq. (3), EF is error fraction, expressed as the precision of VOCs species, and the setting

211   range can be adjusted from 5 to 20% according to the concentration difference (Buzcu

212   et al., 2006; Song et al., 2007); and c_{ij} is the concentration of species j in sample i:

213
$$U_{ij} = \sqrt{\left(EF \times c_{ij}\right)^2 + (0.5 \times MDL)^2} \qquad (3)$$

214   when the concentration of VOCs in the species is less than the value of the

215   detection limit U_{ij} is calculated using Eq. (4):

216
$$U_{ij} = \left(\frac{5}{6}\right) MDL \qquad (4)$$

217   VOC species and concentration input into PMF were carefully selected to ensure

218   the accuracy of the PMF results. Species were excluded when over 25% of the samples

219   were missing or concentrations values were below the MDL (Gao et al., 2018); VOCs

220   with a short lifetime in the atmosphere were also excluded unless they are source-

221   relative species (Zhang et al., 2014; Shao et al., 2016). After that, retained VOC species

222   were categorized according to the signal-to-noise ratio (S/N) with S/N < 0.2 species

223   categorized as bad, 0.2 < S/N < 2 species categorized as weak; and S/N > 2 species

224   categorized as strong (Shao et al., 2016).

225   We used displacement of factor elements (DISP) to assess PMF modelling

226   uncertainty (for a description, see Paatero et al. (2014)). Q was less than 1% and no

227   swaps occurred for the small est dQ^{max} in DISP. Fpeak values from -2 to 2 were tested

228   to explore the rotational stability of the solutions. Q$_{true}$/Q$_{exp}$ is lowest when Fpeak = 0,

229   so we chose the PMF results for that case (Fig. S2a). After examining 3-8 factors, 20

230   base runs with 5 factors eventually selected to represent final result. We provide an

231   explanation of factor selection in the supplementary materials. Fig. S2(b) includes

232   Q$_{true}$/Q$_{exp}$, Q$_{robust}$/Q$_{exp}$ for factors 3-8. The slopes of these two ratios in changed at five

233   factors, and we found that five factors were more realistic after repeated comparisons

234   of the results at four, five and six factors.

2.3 SOA generation potential

The contributions of VOC species to SOAP were calculated based on the toluene weighted mass contributions (TMC) method (Derwent et al., 2010). The methodology for calculating SOAP is as follows:

$$SOAPF_i = \frac{VOCs\ component\ i\ to\ SOA\ mass\ concentration\ increments}{Toluene\ to\ SOA\ mass\ concentration\ increment} \times 100 \quad (5)$$

$SOAPF_i$ for each VOC is taken from the literature (Derwent et al., 2010). The SOAP was estimated by multiplying the $SOAPF_i$ value by the concentration of individual VOC species. The SOAP calculations through each VOC are as follows:

$$SOAP = \sum E_i \times SOAPF_i \quad (6)$$

E_i is the concentration of species i.

3. Results and discussion

3.1 Overview of variation in pollutants and meteorological parameters

Figure 1 shows the time series of meteorological parameters, TVOCs, O_3, NO_x, SO_2, CO and $PM_{2.5}$ during the observed periods. Low WS and Temperature were found with an average value of 1.3 ± 0.6 m/s and 5.0 ± 2.5 °C, respectively, during the entire period, comparable with observations at the same site in 2021 (Lai et al., 2024). A total of 62 days of valid data was acquired with the daily average concentration of $PM_{2.5}$ ranging from 53 to 239 µg/m³, with the average value of 111 ± 45 µg/m³. The concentration of TVOCs ranged from 15.6 to 57.1 ppbv with an average of 36.1 ± 21.0 ppbv, higher than the same period in last year (27.9 ± 12.7 ppbv, Lai et al., 2024). During the observation period, the average values of T, WS and RH were 5.0 ± 2.5 °C, 1.3 ± 0.6 m/s and $38.9 \pm 16.7\%$, respectively.

Previous studies have shown that meteorological factors such as low wind speed, high relative humidity, and low precipitation are responsible for the increase in particulate matter pollution in Zhengzhou in winter (Duan et al., 2019). Our analysis of the correlation between different pollutants and meteorological conditions during

the pollution period showed that $PM_{2.5}$, TVOCs and NO_x were positively correlated with relative humidity (Fig. S3), which is consistent with the results of some previous studies (Wang et al., 2019). The comparisons of average concentrations of different periods between different periods are presented in Tables 1 and 2. The comparison between polluted and clean days shows that the wind speed is lower than that of clean days and the humidity is higher than that of clean days, which is consistent with the meteorological conditions characterized by the occurrence of polluted days. WS, Temp and RH conditions during infection and recovery periods were generally similar. However, the average concentration of $PM_{2.5}$ during the recovery period was 1.6 times the value during the infection period. Furthermore, the concentrations of other pollutants including SO_2, NO_2, CO, and O_3 all showed a similar trend between infection and recovery periods. The TVOCs concentration during the recovery period was 1.2 times the value during the infection period, showing an obvious increase trend after resuming production. A comparison of the meteorological conditions associated with the two pollution processes revealed no discernible trend towards greater susceptibility to pollution. However, the concentrations of pollutants in Case 2 were significantly higher than in Case 1, a trend that is most likely attributable to the resumption of production activities and increased emissions during Case 2. Decreased trends of air pollutants were found in other studies before and after the outbreak of the novel coronavirus (COVID-19) in early 2020 (Qi et al., 2021; Wang et al., 2021).
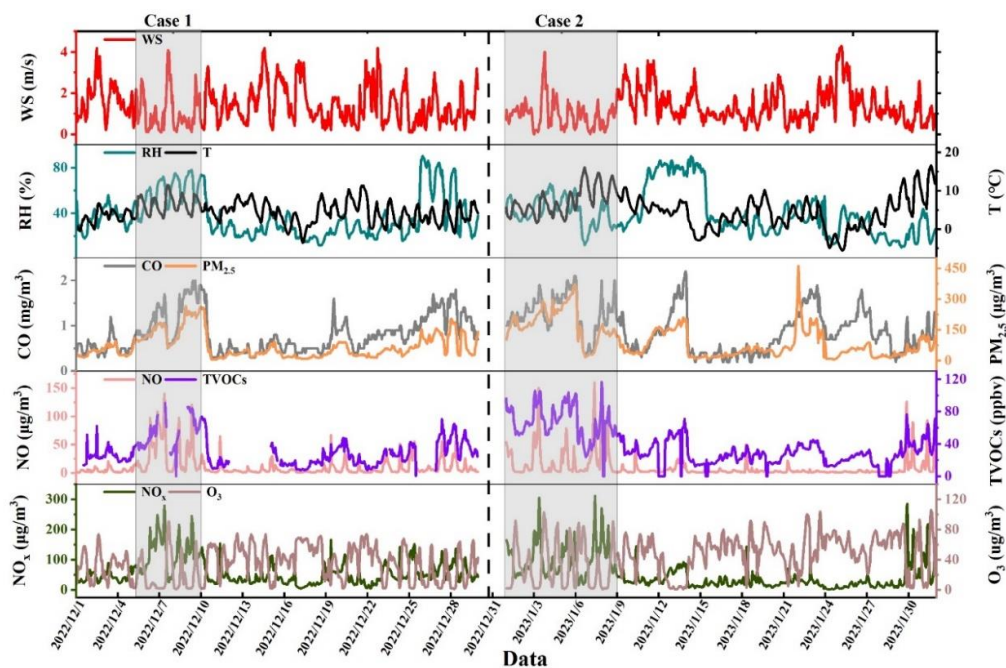
Fig. 1. Time series of WS, T, RH, CO, $PM_{2.5}$, NO, TVOCs, NO_x and O_3 during the observation

288   period.

289   The shadow section in Fig. 1 represents two haze pollution events during the

290   monitoring period. A pollution event is determined when the daily average

291   concentration of $PM_{2.5}$ exceeds 75 μg/m^3 (China's II-level standard) for at least three

292   consecutive days. Case 1 (December 5 to December 10 with daily average $PM_{2.5}$ =

293   142.5 μg/m^3) and Case 2 (January 1 to January 8 with daily average $PM_{2.5}$ = 181.5

294   μg/m^3) were selected as they represent the pollution events in infection and recovery

295   periods, respectively, due to their long duration and high pollution levels. Any day with

296   a $PM_{2.5}$ concentration lower than 35 μg/m^3 (China's I-level standard) is considered as

297   Clean days.
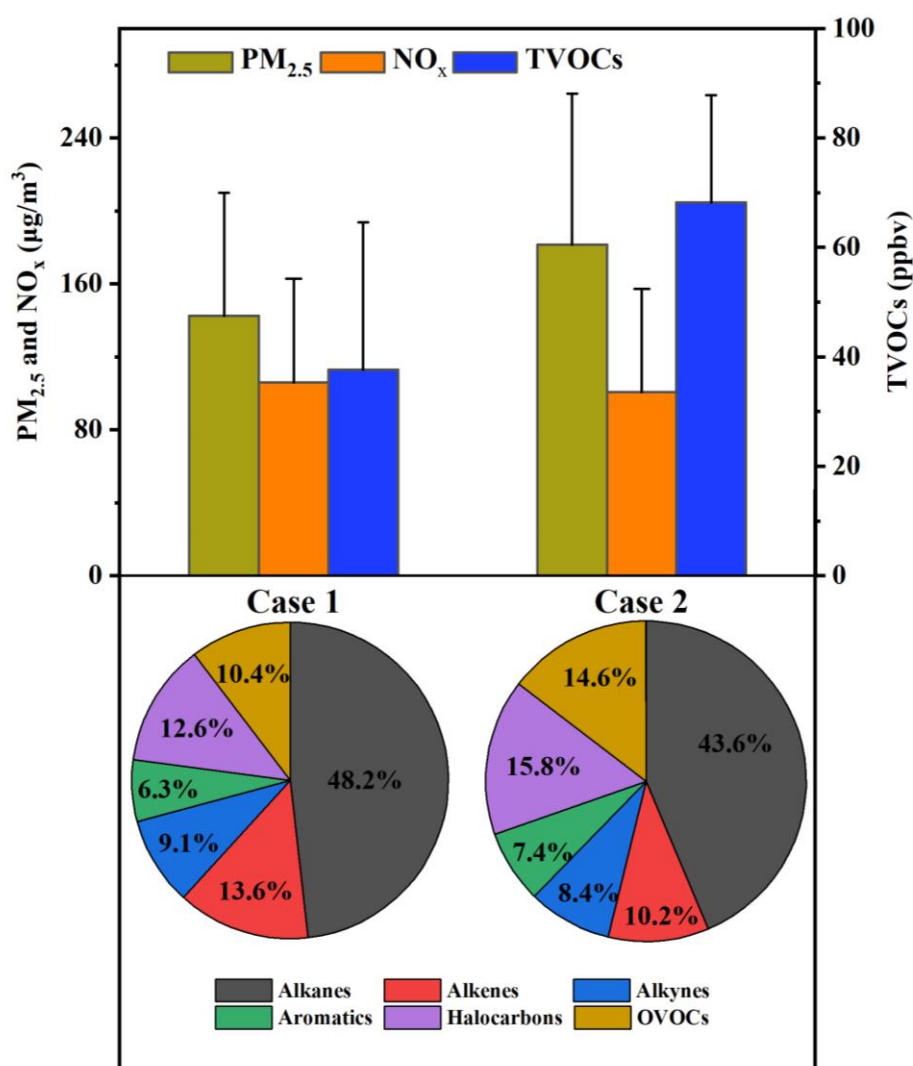
298

299   Fig. 2. The concentration of $PM_{2.5}$, NO_x, TVOCs and the composition ratio of VOCs in Case 1 and

300   Case 2.

301   As for the two representative pollution processes (Case 1 during the infection

302   period and Case 2 during the recovery period), the concentration of TVOCs in Case 1

303   and Case 2 were 48.4 ± 20.4 and 67.6 ± 19.6 ppbv (Fig. 2), respectively, increased by

304   63% and 188% compared with values during clean days. The average concentrations

305   of $PM_{2.5}$ and TVOCs during Case 2 were 1.3 and 1.8 times the values in Case 1. The

306   highest volume contributions of alkanes were found both in Case 1 (48%) and Case 2

307   (44%), consistent with the results in the Yangtze River Delta region (36-43%, Liu et al.,

308   2023). While alkenes exhibited higher volume percentages of 13% in Case 1, followed

309   by halogenated hydrocarbon (12%) and OVOCs (10%). Higher volume percentages of

310   alkanes and alkenes in Case 1 were similar to the results in the gasoline evaporation

311   site in winter (Niu et al., 2022). Equivalent volume contribution of halogenated

312   hydrocarbon and OVOCs (15%) were found in Case 2, followed by alkenes (10%).

313   Although aromatic hydrocarbons have the lowest volumetric contribution (6% in Case

314   1 and 7% in Case 2), they show the largest increase from clean days to pollution.

315   Table 1 The average concentrations of meteorological parameters and pollutants during different
316   processes.

Category	Entire process (2022.12.1-2023.1.31)	Infection period (2022.12.1-2022.12.31)	Recovery period (2023.1.1-2023.1.31)	Case 1 (2022.12.5-2022.12.10)	Case 2 (2023.1.1-2023.1.10)	Clean Days
	N = 62 days	N = 31 days	N = 31 days	N = 6 days	N = 8 days	N = 8 days
WS (m/s)	1.3 ± 0.6	1.4 ± 0.6	1.3 ± 0.6	1.2 ± 0.9	0.9 ± 0.7	1.4 ± 0.8
T (°C)	5.0 ± 2.5	4.7 ± 1.7	5.4 ± 3.1	6.1 ± 2.2	7.4 ± 3.5	4.1 ± 3.0
RH (%)	38.9 ± 16.7	37.6 ± 15.5	40.2 ± 18.2	55.7 ± 14.7	42.0 ± 12.1	29.5 ± 18.1
TVOCs (ppbv)	36.1 ± 21.0	31.9 ± 18.1	39.8 ± 22.4	37.6 ± 27.0	68.2 ± 19.6	22.7 ± 11.1
SO_2 (µg/m³)	11.4 ± 2.7	10.2 ± 2.8	12.7 ± 2.3	11.0 ± 3.7	16.2 ± 6.1	6.5 ± 2.5
NO_2 (µg/m³)	47.2 ± 10.0	46.8 ± 8.6	47.8 ± 11.7	62.7 ± 20.5	65.0 ± 21.3	20.8 ± 15.9
CO (mg/m³)	0.9 ± 0.2	0.8 ± 0.2	1.1 ± 0.2	1.2 ± 0.5	1.3 ± 0.4	0.5 ± 0.2
O_3 (µg/m³)	34.9 ± 6.0	31.1 ± 4.5	39.0 ± 4.6	21.8 ± 23.7	32.5 ± 29.6	52.6 ± 18.4
$PM_{2.5}$ (µg/m³)	111.5 ± 45.1	86.6 ± 34.6	138.3 ± 39.6	142.5 ± 67.4	181.5 ± 82.7	23.8 ± 16.8

317   Table 2 Concentration of VOC species during different processes (ppbv).

Category	Entire process	Infection period	Recovery period	Case 1	Case 2	Clean days
TVOCs	36.1 ± 21.0	31.9 ± 18.1	39.8 ± 22.4	48.4 ± 20.4	67.6 ± 19.6	17.5 ± 9.5
alkanes	16.8 ± 9.2	15.0 ± 8.4	18.4 ± 9.5	23.1 ± 10.0	29.5 ± 8.4	9.2 ± 5.6
alkenes	4.1 ± 2.7	3.8 ± 2.6	4.4 ± 2.7	6.5 ± 2.9	7.0 ± 2.6	1.7 ± 1.3
alkynes	3.1 ± 2.0	2.7 ± 1.7	3.4 ± 2.1	4.3 ± 2.0	5.8 ± 1.9	1.3 ± 0.8
aromatics	2.1 ± 2.0	1.8 ± 1.5	2.3 ± 2.2	3.0 ± 1.8	4.9 ± 2.8	0.7 ± 0.5

halogenated hydrocarbon	5.4 ± 3.3	4.4 ± 2.3	6.2 ± 3.8	6.0 ± 1.9	10.7 ± 3.6	2.7 ± 1.4
OVOCs	4.6 ± 3.2	3.5 ± 2.7	5.1 ± 3.5	5.0 ± 2.4	9.7 ± 2.8	1.9 ± 1.1

318 **3.2 Source Analysis of VOCs**

319   Specific VOC ratios can be used for initial source identification of VOCs and

320 determination of photochemical ages of air masses (Monod et al., 2001; An et al., 2014;

321 Li et al., 2019). In this study, the ratios of toluene/benzene (T/B), isopentane/n-pentane,

322 isobutane/n-butane, and m/p-xylene/ethylbenzene (X/E) were selected to initially

323 identify the potential sources of VOCs (Fig. 3). Concentrations of selected pollutants

324 and ratios used are shown in Table S1.

325   Toluene-to-benzene ratio (T/B ratio) was widely used to assess the relative

326 importance of different sources. Specifically, T/B ratio with the value of 1.3–3.0 was

327 observed in vehicle emissions for vehicles with different fuel types (Schauer et al., 2002;

328 Wang et al., 2015). The reported T/B ratio for combustion processes was between 0.13

329 and 0.7 (Li et al., 2011; Wang et al., 2014). The average T/B value for the entire period

330 was 1.0, indicating that both traffic emissions and combustion are significant sources

331 of VOCs.

332   The isopentane/n-pentane concentration ratios of 0.6-0.8 represent mainly coal

333 combustion emissions, ratios of 0.8-0.9 represent liquefied petroleum gas (LPG)

334 emissions, 2.2-3.8 represent vehicle exhaust emissions, and 1.8-4.6 represent fuel

335 evaporation (Conner et al., 1995; Liu et al., 2008; Li et al., 2019). The overall ratio of

336 isopentane/n-pentane is 1.4, indicating that pentane is mainly derived from the

337 combined effects of liquid petrol and fuel evaporation.

338   Isobutane/n-butane concentration ratios of 0.2-0.3 represent vehicle emissions,

339 0.4-0.6 represent LPG usage, and 0.6-1.0 represent natural gas emissions (Russo et al.,

340 2010; Zheng et al., 2018). The ratio of isobutane/n-butane in this study was 0.50, which

341 suggests that the VOC concentrations at the observation sites are influenced by natural

342 gas emissions (Shao et al., 2016; Zeng et al., 2023).

343   The ratio of X/E can be used to infer the photochemical age of the air mass. X/E

344 ratios around 2.5-2.9 are typical of urban areas, indicating that VOCs are mainly from

345 the urban area (fresh air mass) (Kumar et al., 2018). When this ratio is significantly

346 lower than 3, it indicates that VOCs are mainly transported from distant sources (aging

347 air masses) (Kumar et al., 2018). The average X/E value in this study was 2.0 (Fig.

348 3(d)), indicating low photochemical activity and aging of the air mass at the observation

349 site. Potential source analyses also indicate that air masses are affected by long-range
350 transport (Fig. S4).
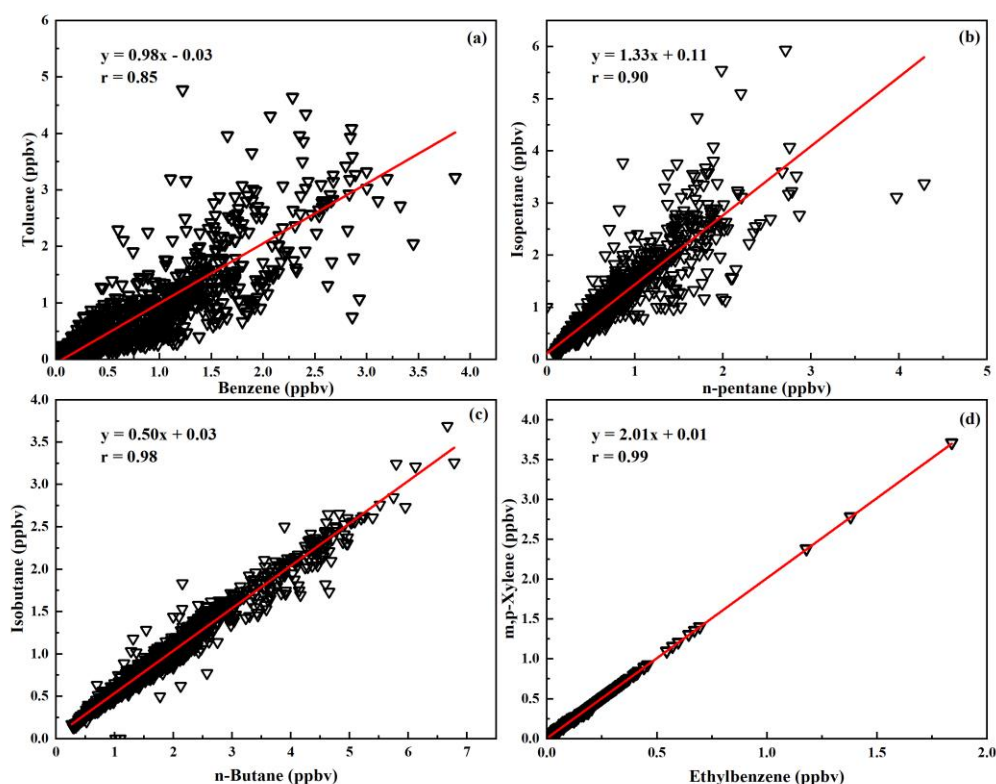
351

352 Fig. 3. Correlation analysis between specific VOC species.

353 Figure 4 shows the chemical profiles of individual VOCs resolved by the PMF
354 model during the entire observation period. These five factors eventually selected as
355 potential sources for the observed VOCs are: (1) Fuel evaporation; (2) Solvent usage;
356 (3) Vehicular emission; (4) Industrial source; and (5) Combustion. These 5 factors have
357 been commonly reported before, e.g., in Shijiazhuang, northern China (Guan et al, 2023)
358 and in Beijing (Cui et al., 2022).

359 Alkanes of C4-C6 substances were predominant in factor 1, including 2-
360 methylpentane, 3-methylpentane, isobutane, n-butane, isopentane and n-pentane from
361 oil and gas (Xiong et al., 2020). Fig. S5 shows that emissions from this source peak at
362 midday, when fuel volatilization is high, The CPF plot shows that south-east is the
363 dominant direction at wind speeds of less than 2 m/s (Fig. 5a). Therefore, factor 1 was
364 identified as the source of oil and gas volatilization.

365 The contribution of benzene, toluene, methylene chloride, 1,2-dichloroethane and
366 ethyl acetate was high in factor 2. It has been shown that benzene, toluene, ethylbenzene,

367 and xylene is an important component in the use of solvents (Li et al., 2015); methylene
368 chloride is often used as a chemical solvent, while esters are mostly used as industrial
369 solvents or adhesives (Li et al., 2015). Factor 2 is determined to be solvent usage source.
370 The CPF plot shows that due east is the main emission direction at wind speeds less
371 than 2 m/s and southeast is the main source at wind speeds greater than 2 m/s (Fig. 5b).

372   Factor 3 contains predominantly C3-C8 alkanes, olefins and alkynes, and
373 relatively high concentrations of benzene. These substances are usually emitted by
374 industrial processes (Shao et al., 2016), so Factor 4 is defined as an industrial source.
375 The CPF plots indicate that a local source at low wind speeds is the dominant sources
376 (Fig. 5c).

377   Factor 4 is characterized by relatively high levels of C2-C6 low-carbon alkanes
378 (ethane, propane, isopentane, n-pentane, isobutane and n-butane), olefins (ethylene and
379 propylene), and benzene and toluene, which are important automotive exhaust tracers
380 (Song et al., 2021; Zhang et al., 2021b). Ethylene and propylene are important
381 components derived from vehicle-related activities. Previous studies of VOCs in
382 Zhengzhou have shown a high percentage of VOCs emitted from gasoline vehicles,
383 with the main source of alkanes being on-road mobile sources (Bai et al., 2020). The
384 daily variation of this source in Fig. S5 shows a bimodal trend, with peaks occurring in
385 the morning and evening peaks of traffic, consistent with motor vehicle emissions. Fig.
386 5d shows that this source is mainly from the west where wind speeds are below 2 m/s,
387 and in this direction, there are a number of urban arterial roads with high traffic volumes.
388 Therefore, factor 4 was defined as vehicular emission source.

389   The highest contribution to factor 5 is chloromethane (62%). Benzene (46%) and
390 acetylene (41%) also contribute highly to factor 5. Chloromethane is the key tracer for
391 biomass combustion and acetylene is the key tracer for coal combustion (Xiong et al.,
392 2020). Therefore, factor 5 is defined as a combustion source. The CPF plot shows that
393 at wind speeds below 2 m/s, the north-east direction is the dominant source direction
394 (Fig. 5e).

395
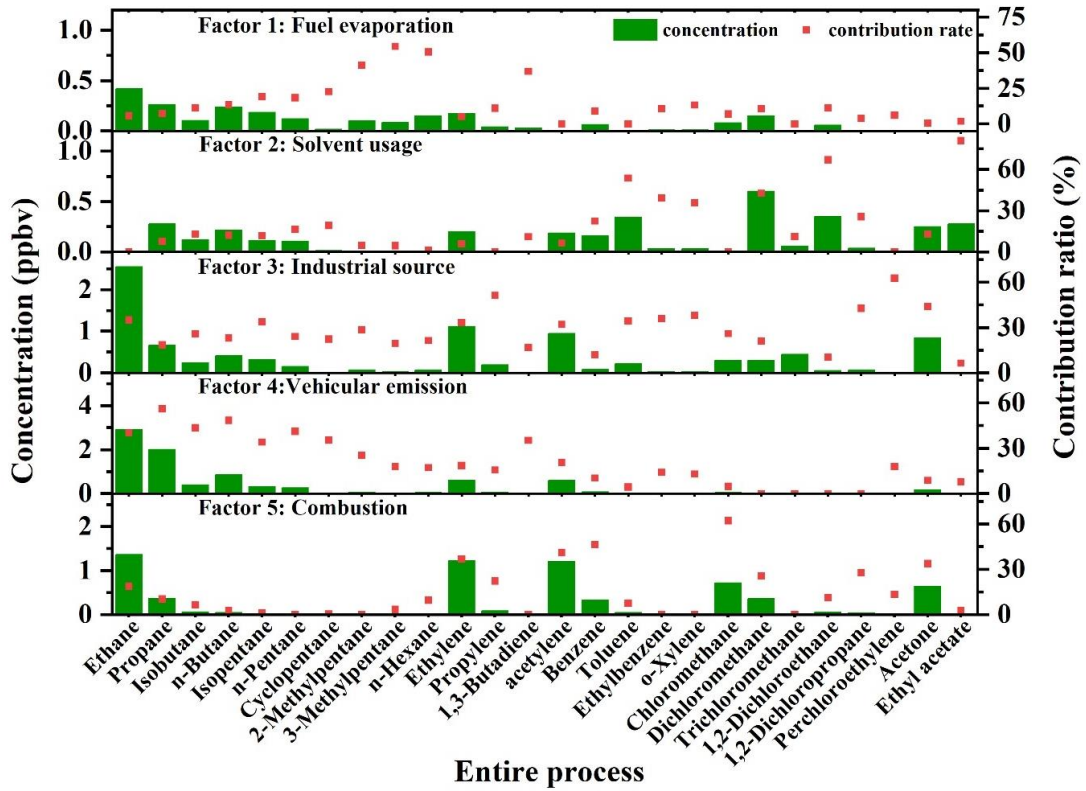
Fig. 4. Concentration of VOC species in each factor and contribution to each source.
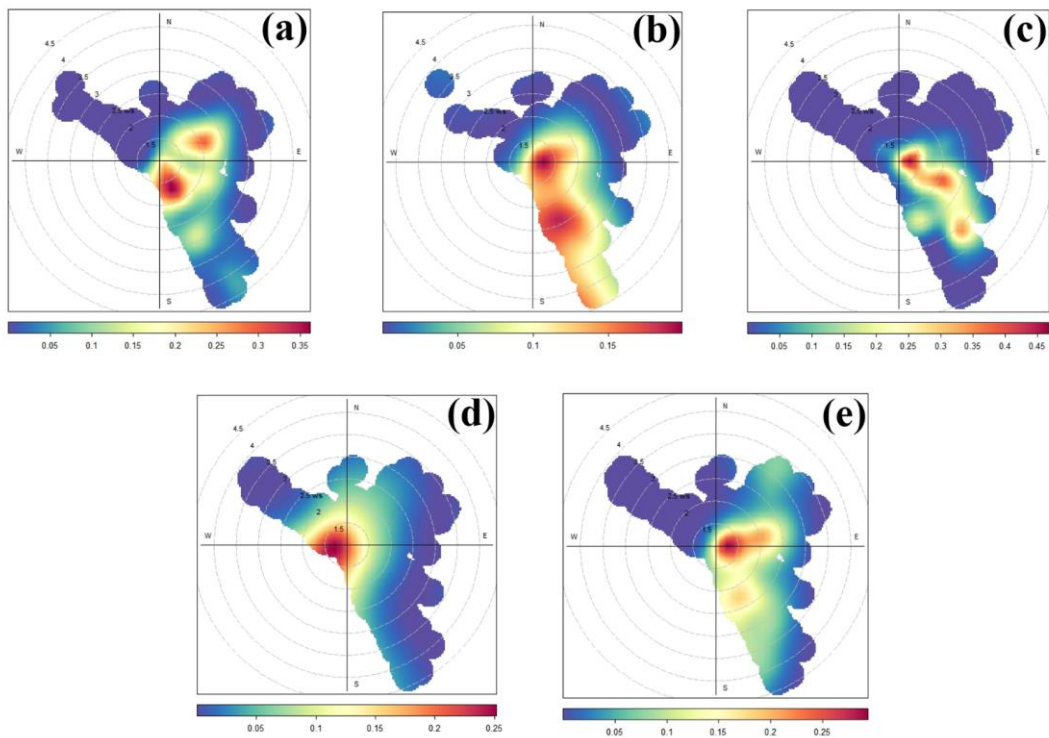
397

398   Fig. 5. CPF plots of five VOCs sources obtained using the PMF model.

401   Fig. S6 compares the differences in PMF source profiles between the Omicron

402   infection period and the recovery period, as well as between the pollution day and the

403   clean day. We present the concentrations of the five main VOCs in all five factors in

404   Table S2. Ethane (vehicular emission), 2-methylpentane (fuel evaporation), benzene

405   (industry source), chloromethane (combustion), and ethyl acetate (solvent usage) were

406   selected as tracers for five sources. Ethane concentration in Case 2 (5.9 ppbv) is much

407   higher than in other processes, and ethane concentration during the recovery period (3.4

408   ppbv) is also higher than during the infection period (2.4 ppbv), which may to some

409   extent reflect increased vehicular emissions during the recovery period.

410   Concentrations of most species were significantly higher during the recovery

411   period than during the infection period. The representative pollution processes in both

412   periods showed the same results as well, with a 79% higher concentration of TVOCs in

413   Case 2 (65.1 ppbv) compared to Case 1 (36.3 ppbv) (Fig. 6). While in Case 1 industry

414   was the dominant source of VOCs, by Case 2 motorized sources reached a

415   concentration value of 21.2 ppbv, accounting for 33% of the observed VOCs, and

416   became the dominant source of emissions. This is consistent with the fact that people's

417   mobility activities have increased after the epidemic has entered the recovery period.

418   As a group of VOCs species with the highest concentration share, ethane and propane

419   contributed more to the clean days motor vehicle source than other processes, which

420   also resulted in a 34% clean days motor vehicle source share.
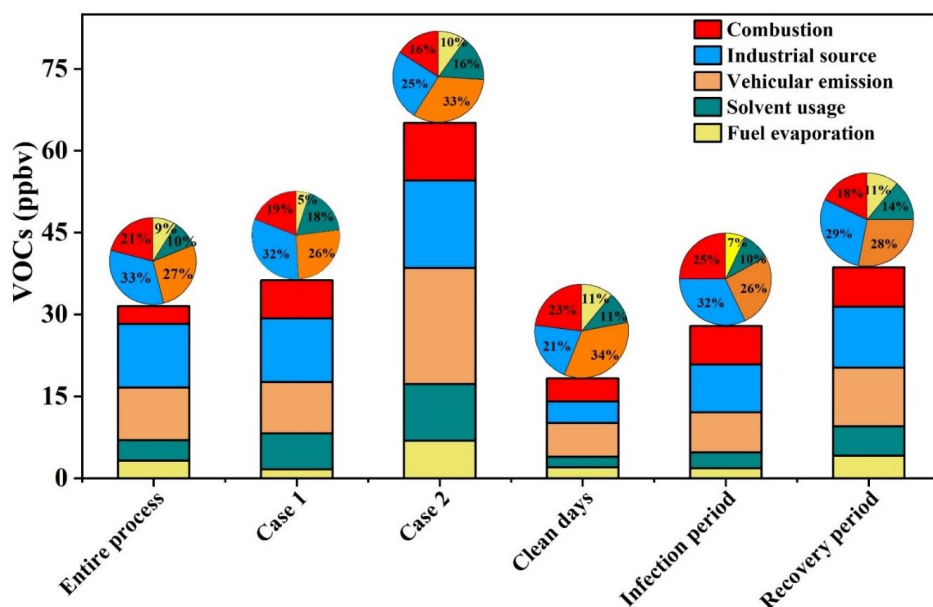
421

422   Fig. 6. Contribution of each to VOCs for different processes.

423 **3.3 SOAP**

424   VOCs are estimated to contribute about 16−30% or more of PM$_{2.5}$ by mass through

425 SOA production (Huang et al., 2014). Therefore, by calculating the SOAP value, the

426 influence of different sources on PM$_{2.5}$ production can be reflected to a certain extent.

427   We have included quantitative analysis for SOAP as well. Fig. 7 shows the SOAP

428 concentrations and contribution rates of the top ten species throughout the entire

429 process, during two pollution processes, and clean days. The top ten species all reached

430 close to 100% of the total SOAP contribution, with Case 1 reaching 98%. In each

431 process, the composition of the top ten substances is essentially the same. Aromatic

432 hydrocarbons contributed the most, with BTEX always occupying the top five positions

433 and toluene the most. The SOAP values of the top ten contributing species for the two

434 polluting processes are shown in Tables S3 and S4. Toluene, the highest contributing

435 species, reached a SOAP value of 49.4 μg/m^3 in the most polluted Case 2, which was

436 3.2 times higher than the SOAP sum of all species on the clean day (15.5 μg/m^3). The

437 SOAP value for Case 1, which is also a contaminated process, was 67 μg/m^3, and the

438 main species (m/xylene: 9.8 μg/m^3, benzene: 8.5 μg/m^3) including toluene (34.6 μg/m^3)

439 were lower than those for Case 2 (m/xylene: 19.4 μg/m^3, benzene: 13.4 μg/m^3).

440
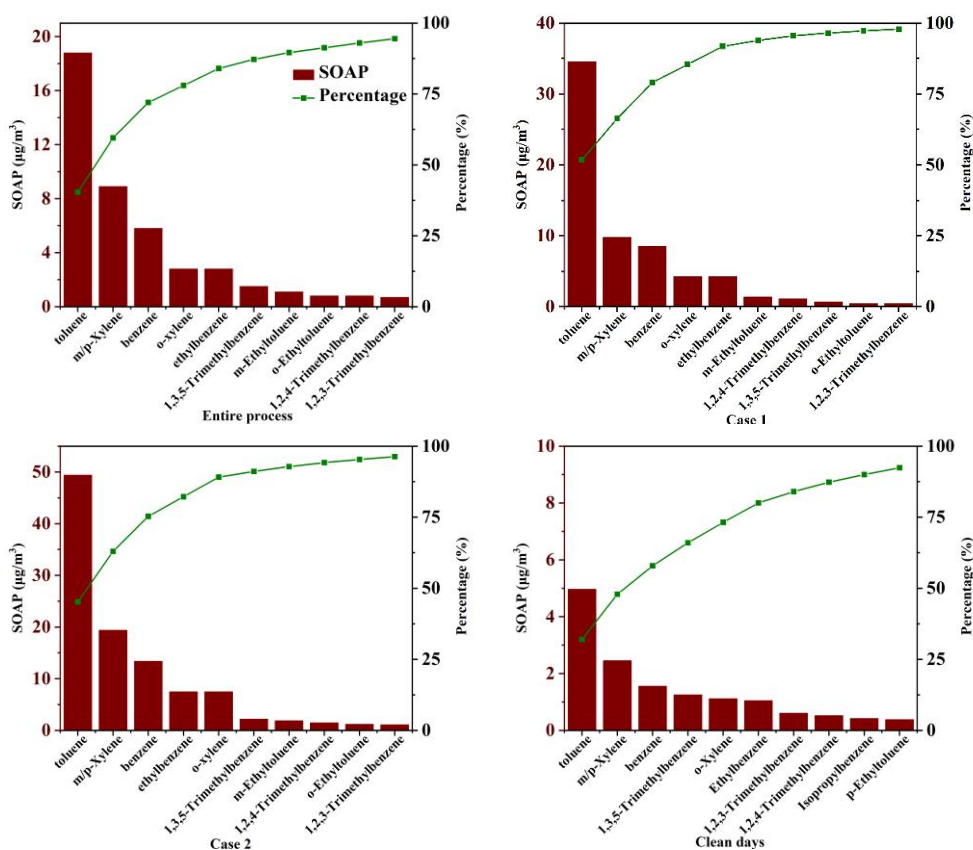
442   Figure 8 shows the SOAP calculated after source resolution of the two pollution

443   processes by PMF for clean days, respectively. In Case 1, industrial source is the

444   dominant source with a contribution ratio of 63%. In Case 2, the pollution sources

445   exhibit a more evenly distributed contribution, where the solvent usage and fuel

446   evaporation sources emerge as the primary contributors to SOAP, with their respective

447   contribution levels rising to 32% and 26%. Case 1 was during the infection period,

448   when social activities had not yet returned to normal. In Case 2, when society had

449   basically returned to normal, the increase in emissions from various sources resulted in

450   a more balanced distribution of SOAP contributions and caused more severe PM$_{2.5}$

451   pollution. In addition, a few days before Case 2, the Zhengzhou Municipal People's

452   Government   initiated   the   Heavy   Pollution   Weather   Level   II   response

453   (https://sthjj.zhengzhou.gov.cn/tzgg/7037130.jhtml) and introduced control measures

454   for emissions from industrial and mobile sources, which resulted in a significant

455   reduction of SOAP levels from industrial and motorized sources in Case 2. The clean

456   day result with a SOAP of 8.8 μg/m^3 also indicates that industrial and solvent usage

457   sources are the most dominant SOAP sources. The primary sources of aromatic

458   compounds, which are the most significant contributors to SOAP, are solvent usage and

459   industrial process emissions. This finding aligns with the results of other studies (Wu

460   et al., 2017). Consequently, it is imperative to implement measures to reduce PM$_{2.5}$

461   pollution by regulating emissions from industrial and solvent usage sources.
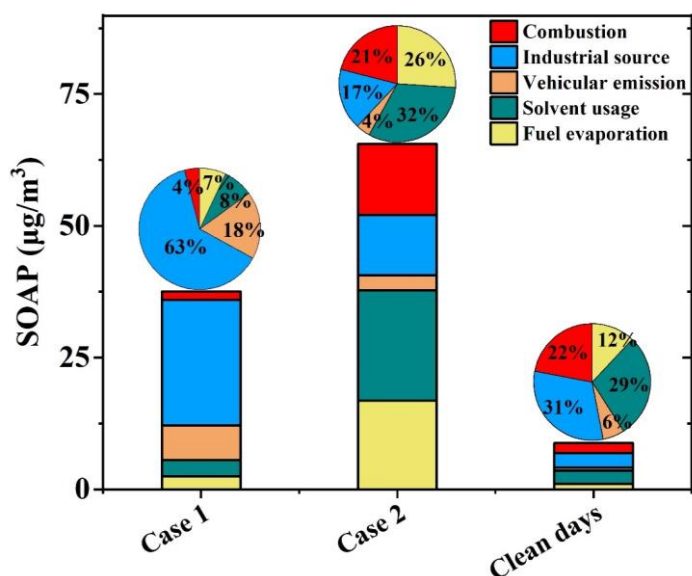
462

463   Fig. 8. SOAP value and contribution ratio of each process

464

4. Conclusions

Continuous observation of VOCs during the infection of the Omicron epidemic was carried out at an urban site in polluted Zhengzhou from December 1, 2022, to January 31, 2023. The daily average concentration of $PM_{2.5}$ ranged from 53.5 to 239.4 $\mu g/m^3$ with an average value of 111.5 ± 45.1 $\mu g/m^3$ during the whole period. The concentration of TVOCs ranged from 15.6 to 57.1 ppbv with an average of 36.1 ± 21.0 ppbv, higher than the same period in last year (27.9 ± 12.7 ppbv, Lai et al., 2024). Two representative contamination processes were identified (Case 1 during the infection period and Case 2 during the recovery period). The concentration of TVOCs in Case 1 and Case 2 were 48.4 ± 20.4 and 67.6 ± 19.6 ppbv, respectively, increased by 63% and 188% compared with values during clean days. The average concentrations of $PM_{2.5}$ and TVOCs during Case 2 were 1.3 and 1.8 times of the values in Case 1. This is consistent with the observed increase in pollutant emissions following the return to normal social life from the period of Omicron infection. The highest volume contributions of alkanes were found both in Case 1 (48%) and Case 2 (44%). Though the volume contribution of aromatics were the lowest (6% in Case 1 and 7% in Case 2), the highest increase ratio was found from clean days to polluted episodes. Low wind speed and high humidity were the main meteorological reasons for the occurrence of pollution. Analyzing the sources of VOCs revealed that VOCs were found to be affected by a combination of local emissions and regional transport. The primary sources of atmospheric VOCs in Zhengzhou were identified as industrial emissions (32%), vehicle emissions (27%), and combustion (21%). Significant discrepancies were observed in the sources of VOCs between the two pollution processes. In Case 1, industrial emissions constituted the primary source of VOCs, accounting for 32% of the total VOC concentration. In contrast, in Case 2, the proportion of vehicle emissions increased to 33%, representing the primary source of VOCs.

A further analysis of the effect of VOCs on SOA generation reveals that aromatic compounds are the primary contributors to SOAP, with BTEX being the predominant contributor throughout the period. The SOAP values reached 37.6 and 65.6 $\mu g/m^3$ in Case 1 and Case 2, respectively. In Case 1, the greatest contribution to SOAP was made by industrial sources (63%, 23.8 $\mu g/m^3$), while vehicular sources, which constituted the second most important source, accounted for only 18%. In Case 2, the contribution of each VOC source was more evenly distributed, with solvent use sources and fuel

evaporation sources representing the primary contributors to SOAP, accounting for 32% (20.9 μg/m³) and 26% (16.8 μg/m³), respectively. The SOAP result for the clean day was 8.8 μg/m³, with industrial sources and solvent use still being the primary contributors. Therefore, the industrial and solvent use sectors are the predominant sources of pollutants during this observation. The aforementioned results substantiate the considerable impact of elevated emissions from all sources on the exacerbation of pollution following the conclusion of the Omicron infection.

Acknowledgments:

This research was supported by the Natural Science Foundation of Henan Province (232300421395) and the National Key Research and Development Program of China (2017YFC0212400).

References

An, J., Zhu, B., Wang, H., Li, Y., Lin, X., and Yang, H.: Characteristics and source apportionment of VOCs measured in an industrial area of Nanjing, Yangtze River Delta, China, Atmospheric Environment, 97, 206-214, https://doi.org/10.1016/j.atmosenv.2014.08.021, 2014.

Bai, L., Lu, X., Yin, S., Zhang, H., Ma, S., Wang, C., Li, Y., and Zhang, R.: A recent emission inventory of multiple air pollutant, $PM_{2.5}$ chemical species and its spatial-temporal characteristics in central China, Journal of Cleaner Production, 269, 122114, https://doi.org/10.1016/j.jclepro.2020.122114, 2020.

Buzcu, B. and Fraser, M. P.: Source identification and apportionment of volatile organic compounds in Houston, TX, Atmospheric Environment, 40, 2385-2400, https://doi.org/10.1016/j.atmosenv.2005.12.020, 2006.

Conner, T. L., Lonneman, W. A., Seila, R.L.: Transportation-related volatile hydrocarbon source profiles measured in atlanta, Journal of the Air & Waste Management Association, 45 (5), 383-394, https://doi.org/10.1080/10473289.1995.10467370, 1995.

Cui, L., Wu, D., Wang, S., Xu, Q., Hu, R., and Hao, J.: Measurement report: Ambient volatile organic compound (VOC) pollution in urban Beijing: characteristics, sources, and implications for pollution control, Atmospheric Chemistry and Physics, 22, 11931-11944, https://doi.org/10.5194/acp-22-11931-2022, 2022.

Derwent, R. G., Jenkin, M. E., Utembe, S. R., Shallcross, D. E., Murrells, T. P.,

and Passant, N. R.: Secondary organic aerosol formation from a large number of reactive man-made organic compounds, Science of the Total Environment, 408, 3374-3381, https://doi.org/10.1016/j.scitotenv.2010.04.013, 2010.

Duan, S., Jiang, N., Yang, L., Zhang, R.: Transport Pathways and Potential Sources of $PM_{2.5}$ During the Winter in Zhengzhou, Environmental Science, Jan 8;40(1):86-93, https://doi.org/10.13227/j.hjkx.201805187, 2019.

Gao, J., Zhang, J., Li, H., Li, L., Xu, L., Zhang, Y., Wang, Z., Wang, X., Zhang, W., Chen, Y., Cheng, X., Zhang, H., Peng, L., Chai, F., and Wei, Y.: Comparative study of volatile organic compounds in ambient air using observed mixing ratios and initial mixing ratios taking chemical loss into account – A case study in a typical urban area in Beijing, Science of the Total Environment, 628-629, 791-804, https://doi.org/10.1016/j.scitotenv.2018.01.175, 2018.

Guan, Y., Liu, X., Zheng, Z., Dai, Y., Du, G., Han, J., Hou, L. a., and Duan, E.: Summer O_3 pollution cycle characteristics and VOCs sources in a central city of Beijing-Tianjin-Hebei area, China, Environmental Pollution, 323, 121293, https://doi.org/10.1016/j.envpol.2023.121293, 2023.

Huang, R., Zhang, Y., Bozzetti, C. et al.: High secondary aerosol contribution to p articulate pollution during haze events in China, Nature, 514 (7521), 218−22, https://d oi.org/10.1038/nature13774, 2014.

Hui, L., Liu, X., Tan, Q., Feng, M., An, J., Qu, Y., Zhang, Y., Deng, Y., Zhai, R., a nd Wang, Z.: VOC characteristics, chemical reactivity and sources in urban Wuhan, ce ntral China, Atmospheric Environment, 224, 117340, https://doi.org/10.1016/j.atmose nv.2020.117340, 2020.

Jensen, A., Liu, Z., Tan, W., Dix, B., Chen, T., Koss, A., Zhu, L., Li, L., de Gouw, J.: Measurements of volatile organic compounds during the COVID-19 lockdown in Changzhou, China, Geophysical research letters, 48(20), https://doi.org/10.1029/2021 GL095560, 2021.

Jiang, N., Hao, X., Hao, Q., Wei, Y., Zhang, Y., Lyu, Z., Zhang, R.: Changes in se condary inorganic ions in $PM_{2.5}$ at different pollution stages before and after COVID-1 9 control, Environmental Science, 44(5), 2430-2440, https://doi.org/10.13227/j.hjkx.2 02206170, 2023.

Kumar, A., Singh, D., Kumar, K., Singh, B. B., and Jain, V. K.: Distribution of VOCs in urban and rural atmospheres of subtropical India: Temporal variation, source attribution, ratios, OFP and risk assessment, Science of the Total Environment, 613-614,

564   492-501, https://doi.org/10.1016/j.scitotenv.2017.09.096, 2018.

565   Lai, M., Zhang, D., Yin, S., Song, X., and Zhang, R.: Pollution characteristics,
566   source apportionment and activity analysis of atmospheric VOCs during winter and
567   summer pollution in Zhengzhou City, Environmental Science, 4108, 3500-3510,
568   https://doi.org/10.13227/j.hjkx.202001133, 2024.

569   Li, B., Ho, S. S. H., Gong, S., Ni, J., Li, H., Han, L., Yang, Y., Qi, Y., and Zhao,
570   D.: Characterization of VOCs and their related atmospheric processes in a central
571   Chinese city during severe ozone pollution periods, Atmospheric Chemistry and
572   Physics, 19, 617-638, https://doi.org/10.5194/acp-19-617-2019, 2019.

573   Li, J., Deng, S., Tohti, A., Li, G., Yi, X., Lu, Z., Liu, J., and Zhang, S.: Spatial
574   characteristics of VOCs and their ozone and secondary organic aerosol formation
575   potentials in autumn and winter in the Guanzhong Plain, China, Environmental
576   Research, 211, 113036, https://doi.org/10.1016/j.envres.2022.113036, 2022.

577   Li, J., Xie, S. D., Zeng, L. M., Li, L. Y., Li, Y. Q., and Wu, R. R.: Characterization
578   of ambient volatile organic compounds and their sources in Beijing, before, during, and
579   after Asia-Pacific Economic Cooperation China 2014, Atmospheric Chemistry and
580   Physics, 15, 7945-7959, https://doi.org/10.5194/acp-15-7945-2015, 2015.

581   Li, J., Lu, K., Lv, W., Li, J., Zhong, L., Ou, Y., Chen, D., Huang, X., and Zhang,
582   Y.: Fast increasing of surface ozone concentrations in Pearl River Delta characterized
583   by a regional air quality monitoring network during 2006–2011, Journal of
584   Environmental Sciences, 26, 23-36, https://doi.org/10.1016/S1001-0742(13)60377-0,
585   2014.

586   Liu, Y., Li, X., Tang, G., Wang, L., Lv, B., Guo, X., and Wang, Y.: Secondary
587   organic aerosols in Jinan, an urban site in North China: Significant anthropogenic
588   contributions to heavy pollution, Journal of Environmental Sciences, 80, 107-115,
589   https://doi.org/10.1016/j.jes.2018.11.009, 2019.

590   Liu, Y., Shao, M., Fu, L., Lu, S., Zeng, L., and Tang, D.: Source profiles of volatile
591   organic compounds (VOCs) measured in China: Part I, Atmospheric Environment, 42,
592   6247-6260, https://doi.org/10.1016/j.atmosenv.2008.01.070, 2008.

593   Liu, Y., Song, M., Liu, X., Zhang, Y., Hui, L., Kong, L., Zhang, Y., Zhang, C., Qu,
594   Y., An, J., Ma, D., Tan, Q., and Feng, M.: Characterization and sources of volatile
595   organic compounds (VOCs) and their related changes during ozone pollution days in
596   2016   in   Beijing,   China,   Environmental   Pollution,   257,   113599,
597   https://doi.org/10.1016/j.envpol.2019.113599, 2020.

598   Liu, Z., Hu, K., Zhang, K., Zhu, S., Wang, M., and Li, L.: VOCs sources and roles
599   in O_3 formation in the central Yangtze River Delta region of China, Atmospheric
600   Environment, 302, https://doi.org/10.1016/j.atmosenv.2023.119755, 2023.

601   Li, X., Wang, S., Hao, J.: Characteristics of volatile organic compounds (VOCs)
602   emitted from biofuel combustion in China, Environmental Science, 32, 3515-3521,
603   2011.

604   Li, Y., Yin, S., Zhang R., Yu, S., Yang, J., and Zhang, D.: Characteristics and source
605   apportionment of atmospheric VOCs at different pollution levels in winter in an urban
606   area in Zhengzhou, Environmental Science, 4108, 3500-3510,
607   https://doi.org/10.13227/j.hjkx.202001133, 2020.

608   Ma, Q., Wang, W., Wu, Y., Wang, F., Jin, L., Song, Y., Han, Y., Zhang, R., Zhang,
609   D.: Haze caused by NO_x oxidation under restricted residential and industrial activities
610   in a mega city in the south of North China Plain, Chemosphere, Volume 305, 135489,
611   https://doi.org/10.1016/j.chemosphere.2022.135489, 2022.

612   Merino, M., Marinescu, M., Cascajo, A., Carretero, J., Singh, D.: Evaluating the
613   spread of Omicron COVID-19 variant in Spain, Future Generation Computer Systems,
614   149, 547-561, https://doi.org/10.1016/j.future.2023.07.025, 2023.

615   Monod, A., Sive, B. C., Avino, P., Chen, T., Blake, D. R., and Sherwood Rowland,
616   F.: Monoaromatic compounds in ambient air of various cities: a focus on correlations
617   between the xylenes and ethylbenzene, Atmospheric Environment, 35, 135-149,
618   https://doi.org/10.1016/S1352-2310(00)00274-0, 2001.

619   Mozaffar, A., Zhang, Y.-L., Fan, M., Cao, F., and Lin, Y.-C.: Characteristics of
620   summertime ambient VOCs and their contributions to O_3 and SOA formation in a
621   suburban area of Nanjing, China, Atmospheric Research, 240, 104923,
622   https://doi.org/10.1016/j.atmosres.2020.104923, 2020.

623   Mu, L., Feng, C., Li, Y., Li, X., Liu, T., Jiang, X., Liu, Z., Bai, H., and Liu, X.:
624   Emission factors and source profiles of VOCs emitted from coke production in Shanxi,
625   China, Environmental Pollution, 335, 122373,
626   https://doi.org/10.1016/j.envpol.2023.122373, 2023.

627   Niu, Y., Yan, Y., Chai, J., Zhang, X., Xu, Y., Duan, X., Wu, J., and Peng, L.: Effects
628   of regional transport from different potential pollution areas on volatile organic
629   compounds (VOCs) in Northern Beijing during non-heating and heating periods,
630   Science of the Total Environment, 836, 155465,
631   https://doi.org/10.1016/j.scitotenv.2022.155465, 2022.

632   Norris, G., Duvall, R., Brown, S., Bai. S. EPA Positive Matrix Factorization (PMF)
633   5.0 Fundamentals and User Guide. U.S. Environmental Protection Agency, Washington,
634   DC, EPA/600/R-14/108 (NTIS PB2015-105147), 2014.

635   Paatero, P., Eberly, S., Brown, S. G., Norris, G. A.: Methods for estimating
636   uncertainty in factor analytic solutions, Atmospheric Measurement Techniques, Volume
637   7, 781-797, https://doi.org/10.5194/amt-7-781-2014, 2014.

638   Pei, C., Yang, W., Zhang, Y., Song, W., Xiao, S., Wang, J., Zhang, J., Zhang, T.,
639   Chen, D., Wang, Y., Chen, Y., Wang, X.: Decrease in ambient volatile organic
640   compounds during the COVID-19 lockdown period in the Pearl River Delta region,
641   south China, Science of The Total Environment, 823, 153720,
642   https://doi.org/10.1016/j.scitotenv.2022.153720, 2022.

643   Petersen, M. S., Í Kongsstovu, S., Eliasen, E. H., Larsen, S., Hansen, J. L., Vest,
644   N., Dahl, M. M., Christiansen, D. H., Møller, L. F., & Kristiansen, M. F.: Clinical
645   characteristics of the Omicron variant - results from a Nationwide Symptoms Survey
646   in the Faroe Islands, International Journal of Infectious Diseases, 122, 636–643,
647   https://doi.org/10.1016/j.ijid.2022.07.005, 2022.

648   Qi, J., Mo, Z., Yuan, B., Huang, S., Huangfu, Y., Wang, Z., Li, X., Yang, S., Wang,
649   W., Zhao, Y., Wang, X., Wang, W., Liu, K., and Shao, M.: An observation approach in
650   evaluation of ozone production to precursor changes during the COVID-19 lockdown,
651   Atmospheric Environment, 262, 118618,
652   https://doi.org/10.1016/j.atmosenv.2021.118618, 2021.

653   Russo, R. S., Zhou, Y., White, M. L., Mao, H., Talbot, R., and Sive, B. C.: Multi-
654   year (2004–2008) record of nonmethane hydrocarbons and halocarbons in New
655   England: seasonal variations and regional sources, Atmospheric Chemistry and Physics,
656   10, 4909-4929, https://doi.org/10.5194/acp-10-4909-2010, 2010.

657   Sahu, L. K., Tripathi, N., Gupta, M., Singh, V., Yadav, R., Patel, K.: Impact of
658   COVID-19 Pandemic lockdown in ambient concentrations of aromatic volatile organic
659   compounds in a metropolitan city of western India, Journal of geophysical research,
660   Atmospheres : JGR, 127(6), https://doi.org/10.1029/2022JD036628, 2022.

661   Schauer, J., Kleeman, M., Cass, G., Simoneit, B.: Measurement of emissions from
662   air pollution sources.5. C_1-C_{32} organic compounds from gasoline-powered motor
663   vehicles, Environmental Science & Technology, 36, 1169-1180,
664   https://doi.org/10.1021/es0108077, 2002.

665   Shao, P., An, J., Xin, J., Wu, F., Wang, J., Ji, D., and Wang, Y.: Source

apportionment of VOCs and the contribution to photochemical ozone formation during summer in the typical industrial area in the Yangtze River Delta, China, Atmospheric Research, 176-177, 64-74, https://doi.org/10.1016/j.atmosres.2016.02.015, 2016.

Shi, Y., Liu, C., Zhang, B., Simayi, M., Xi, Z., Ren, J., and Xie, S.: Accurate identification of key VOCs sources contributing to O3 formation along the Liaodong Bay based on emission inventories and ambient observations, Science of the Total Environment, 844, 156998, 10.1016/j.scitotenv.2022.156998, 2022.

Singh, B., Sohrab, S., Athar, M., Alandijany, T., Kumari, S., Nair, A., Kumari, S., Mehra, K., Chowdhary, K., Rahman, S., Azhar, E.: Substantial changes in selected volatile organic compounds (VOCs) and associations with health risk assessments in industrial areas during the COVID-19 Pandemic, Toxics, 11, 165, https://doi.org/10.3390/toxics11020165, 2023a.

Singh, B., Singh, M., Ulman, Y., Sharma, U., Pradhan, R., Sahoo, J., Padhi, S., Chandra, P., Koul, M., Tripathi, P., Kumar, D., Masih, J.: Distribution and temporal variation of total volatile organic compounds concentrations associated with health risk in Punjab, India, Case Studies in Chemical and Environmental Engineering, 8, 100417, https://doi.org/10.1016/j.cscee.2023.100417, 2023b.

Song, M., Li, X., Yang, S., Yu, X., Zhou, S., Yang, Y., Chen, S., Dong, H., Liao, K., Chen, Q., Lu, K., Zhang, N., Cao, J., Zeng, L., and Zhang, Y.: Spatiotemporal variation, sources, and secondary transformation potential of volatile organic compounds in Xi'an, China, Atmospheric Chemistry and Physics, 21, 4939-4958, https://doi.org/10.5194/acp-21-4939-2021, 2021.

Song, X., Zhang, D., Li, X., Lu, X., Wang, M., Zhang, B., Zhang, R.: Simultaneous observations of peroxyacetyl nitrate and ozone in Central China during static management of COVID-19: Regional transport and thermal decomposition, Atmospheric Research, Volume 294, 106958, https://doi.org/10.1016/j.atmosres.2023.106958, 2023.

Song, Y., Shao, M., Liu, Y., Lu, S., Kuster, W., Goldan, P., and Xie, S.: Source apportionment of ambient volatile organic compounds in Beijing, Environmental Science & Technology, 41, 4348-4353, https://doi.org/10.1021/es0625982, 2007.

Wang, H., Li, J., Peng, Y., Zhang, M., Che, H., Zhang, X.: The impacts of the meteorology features on PM2.5 levels during a severe haze episode in central-east China, Atmospheric Environment, Volume 197, Pages 177-189, ISSN 1352-2310, https://doi.org/10.1016/j.atmosenv.2018.10.001, 2019.

700   Wang, H., Wang, Q., Chen, J. Chen, C., Huang, C., Qiao, L. Lou, S., Lu, J.: Do
701   vehicular emissions dominate the source of C6–C8 aromatics in the megacity Shanghai
702   of eastern China?, Environmental Science, 27, 290-297, https://doi.org/10.
703   1016/j.jes.2014.05.033, 2015.

704   Wang, M., Lu, S., Shao, M., Zeng, L., Zheng, J., Xie, F., Lin, H., Hu, K., and Lu,
705   X.: Impact of COVID-19 lockdown on ambient levels and sources of volatile organic
706   compounds (VOCs) in Nanjing, China, Science of the Total Environment, 757, 143823,
707   https://doi.org/10.1016/j.scitotenv.2020.143823, 2021.

708   Wang, M., Zeng, L., Lu, S., Shao, M., Liu, X., Yu, X., Chen, W., Yuan, B., Zhang,
709   Q., Hu, M., & Zhang, Z.: Development and validation of a cryogen-free automatic gas
710   chromatograph system (GC-MS/FID) for online measurements of volatile organic
711   compounds, Analytical Methods, 6, 9424, https://doi.org/10.1039/C4AY01855A, 2014.

712   Wang, T., Xue, L., Brimblecombe, P., Lam, Y. F., Li, L., and Zhang, L.: Ozone
713   pollution in China: A review of concentrations, meteorological influences, chemical
714   precursors, and effects, Science of the Total Environment, 575, 1582-1596,
715   https://doi.org/10.1016/j.scitotenv.2016.10.081, 2017.

716   Wu, R., Li, J., Hao, Y., Li, Y., Zeng, L., and Xie, S.: Evolution process and sources
717   of ambient volatile organic compounds during a severe haze event in Beijing, China,
718   Science of the Total Environment, 560-561, 62-72,
719   https://doi.org/10.1016/j.scitotenv.2016.04.030, 2016.

720   Wu, W., Zhao, B., Wang, S., and Hao, J.: Ozone and secondary organic aerosol
721   formation potential from anthropogenic volatile organic compounds emissions in China,
722   Journal of Environmental Sciences, 53, 224-237,
723   https://doi.org/10.1016/j.jes.2016.03.025, 2017.

724   Xiong, Y., Zhou, J., Xing, Z., and Du, K.: Optimization of a volatile organic
725   compound control strategy in an oil industry center in Canada by evaluating ozone and
726   secondary organic aerosol formation potential, Environmental Research, 191, 110217,
727   https://doi.org/10.1016/j.envres.2020.110217, 2020.

728   Yun, L., Li, C., Zhang, M., He, L. and Guo, J.: Pollution characteristics and sources
729   of atmospheric VOCs in the coastal background area of the Pearl River Delta,
730   Environmental Science, 4191-4201, https://doi.org/10.13227/j.hjkx.202101155, 2021.

731   Zeng, X., Han, M., Ren, G., Liu, G., Wang, X., Du, K., Zhang, X., and Lin, H.: A
732   comprehensive investigation on source apportionment and multi-directional regional
733   transport of volatile organic compounds and ozone in urban Zhengzhou, Chemosphere,

734 334, 139001, https://doi.org/10.1016/j.chemosphere.2023.139001, 2023.

735 Zhang, C., Liu, X., Zhang, Y., Tan, Q., Feng, M., Qu, Y., An, J., Deng, Y., Zhai, R.,
736 Wang, Z., Cheng, N., and Zha, S.: Characteristics, source apportionment and chemical
737 conversions of VOCs based on a comprehensive summer observation experiment in
738 Beijing, Atmospheric Pollution Research, 12, 230-241,
739 https://doi.org/10.1016/j.apr.2020.12.010, 2021a.

740 Zhang, D., He, B., Yuan, M., Yu, S., Yin, S., and Zhang, R.: Characteristics,
741 sources and health risks assessment of VOCs in Zhengzhou, China during haze
742 pollution season, Journal of Environmental Sciences, 108, 44-57,
743 https://doi.org/10.1016/j.jes.2021.01.035, 2021b.

744 Zhang, D., Li, X., Yuan, M., Xu, Y., Xu, Q., Su, F., Wang, S., Zhang, R.:
745 Characteristics and sources of nonmethane volatile organic compounds (NMVOCs) and
746 O3–NOx–NMVOC relationships in Zhengzhou, China, Atmosphere Chemistry and
747 Physics, 24, 8549-8567, https://doi.org/10.5194/acp-24-8549-2024, 2024.

748 Zhang, F., Shang, X., Chen, H., Xie, G., Fu, Y., Wu, D., Sun, W., Liu, P., Zhang,
749 C., Mu, Y., Zeng, L., Wan, M., Wang, Y., Xiao, H., Wang, G., and Chen, J.: Significant
750 impact of coal combustion on VOCs emissions in winter in a North China rural site,
751 Science of the Total Environment, 720, 137617,
752 https://doi.org/10.1016/j.scitotenv.2020.137617, 2020.

753 Zhang, J., Sun, Y., Wu, F., Sun, J., and Wang, Y.: The characteristics, seasonal
754 variation and source apportionment of VOCs at Gongga Mountain, China, Atmospheric
755 Environment, 88, 297-305, https://doi.org/10.1016/j.atmosenv.2013.03.036, 2014.

756 Zhang, Z., Yan, X., Gao, F., Thai, P., Wang, H., Chen, D., Zhou, L., Gong, D., Li,
757 Q., Morawska, L., and Wang, B.: Emission and health risk assessment of volatile
758 organic compounds in various processes of a petroleum refinery in the Pearl River Delta,
759 China, Environmental Pollution, 238, 452-461,
760 https://doi.org/10.1016/j.envpol.2018.03.054, 2018.

761 Zheng, H., Kong, S., Xing, X., Mao, Y., Hu, T., Ding, Y., Li, G., Liu, D., Li, S.,
762 and Qi, S.: Monitoring of volatile organic compounds (VOCs) from an oil and gas
763 station in northwest China for 1 year, Atmospheric Chemistry and Physics, 18, 4567-
764 4595, https://doi.org/10.5194/acp-18-4567-2018, 2018.

765 Zheng, J., Zhong, L., Wang, T., Louie, P. K. K., and Li, Z.: Ground-level ozone in
766 the Pearl River Delta region: Analysis of data from a recently established regional air
767 quality monitoring network, Atmospheric Environment, 44, 814-823,

768 https://doi.org/10.1016/j.atmosenv.2009.11.032, 2010.

769 Zhou, Z., Xiao, L., Fei, L., Yu, W., Lin M., Huang, T., Zhang, Z. and Tao J.:

770 Characteristics and sources of VOCs during ozone pollution and non-pollution periods

771 in summer in Dongguan industrial concentration area, Environmental Science, 4497-

772 4505, https://doi.org/10.13227/j.hjkx.202111285, 2022.

773 Zou, Y., Yan, X. L., Flores, R. M., Zhang, L. Y., Yang, S. P., Fan, L. Y., Deng, T.,

774 Deng, X. J., and Ye, D. Q.: Source apportionment and ozone formation mechanism of

775 VOCs considering photochemical loss in Guangzhou, China, Science of the Total

776 Environment, 903, 166191, https://doi.org/10.1016/j.scitotenv.2023.166191, 2023.

777 Zuo, H., Jiang, Y., Yuan, J., Wang, Z., Zhang, P., Guo, C., Wang, Z., Chen, Y., Wen,

778 Q., Wei, Y., Li, X.: Pollution characteristics and source differences of VOCs before and

779 after COVID-19 in Beijing, Science of The Total Environment, 907, 167694,

780 https://doi.org/10.1016/j.scitotenv.2023.167694, 2024.

781